



Studying the best Location and Dimensions of Stilling Basin Pool downstream Hydraulic Structures

Alaa N. El-HAZEK¹, Neveen B. Abdel-Mageed², Abdelazim M. Ali³, and Esraa S. Mahgoub⁴

¹Professor Emeritus, Civil Eng. Dept, Faculty of Engineering at Shoubra, Benha University, Egypt.

¹Orcid ID: 0000-0003-0911-4592

²Assoc. Professor, Civil Eng. Dept, Faculty of Engineering at Shoubra, Benha University, Egypt.

³Assoc. Professor, Hydraulics Research Institute, National Water Research Center, Egypt.

⁴Researcher Assistant, Hydraulics Research Institute, National Water Research Center, Egypt.

نبذة مختصرة

تستخدم أحواض التهدئة بشكل عام لتشتيت الطاقة الهيدروليكية الزائدة عند تصميم المنشآت الهيدروليكية مثل السدود والقناطر والهدارات وما إلى ذلك لمنع حدوث النحر أسفل هذه المنشآت وبالتالي تجنب إهيارها وزيادة عمرها الافتراضي. تركز ورقة البحث على دراسة تأثير الأشكال والأبعاد المختلفة لأحواض التهدئة المصاحبة لحدوث القفزة الهيدروليكية المغمورة أسفل مجرى فتحة بوابة المنشأ المائي لتعظيم كمية الطاقة المشتتة وتقليل النحر. بشكل عام، يبحث هذا البحث الخصائص والمعايير الرئيسية للقفزة الهيدروليكية المغمورة مثل تبديد الطاقة على طول حوض التهدئة وطول القفزة، بالإضافة إلى توزيع السرعات، وسرعة السريان القريبة من القاع على طول حوض التهدئة، ومشكلة النحر على طول مجرى حوض التهدئة. سيتم في هذا البحث إختبار هذه الخصائص في حوض تهدئة مزود ببركة ذات أبعاد مختلفة وعلى أبعاد مختلفة من بوابة المنشأ الهيدروليكي. تم إجراء ثمانية وأربعين إختبار، لكل إختبار من هذه الإختبارات تصرف سريان (Q)، إرتفاع فتحة البوابة (G)، إرتفاع السريان عند (vena contracta) y_1 ، إرتفاع أعماق المياه المترافقة والمتسلسلة conjugate and sequent المصاحبة للقفزة y_2 ، طول القفزة المغمورة (Ls)j، وسوف يتم حساب قيمة أرقام فرويد المصاحب لل Vena- Contracta. تم إجراء البرنامج التجريبي على نموذج معاد تدويره بعرض 0.1 متر وطول 26 متر وعمق 2.1 متر مع مدى تصرف من 60 إلى 90 لتر/ ثانية. تم تطوير معادلات إحصائية لربط طول القفزة المغمورة بالمعاملات المستقلة الأخرى. أخيرا، تم الحصول على مطابقة واضحة للنتائج من تحليل طول القفزة والسرعة وتم تحديد أفضل تصميم لحوض التهدئة.

ABSTRACT

Stilling basins are in common use when designing heading-up hydraulic structures such as dams, barrages, spillways, etc. This paper focuses on studying the effect of different locations and dimensions of stilling basin pools with the submerged hydraulic jump downstream the hydraulic structure sluice gate. Also, this research investigates the main characteristics and parameters of the submerged hydraulic jump such as the energy

dissipation along the stilling basin and the length of the submerged hydraulic jump, in addition to the velocity distribution, the near-bed velocity decay along stilling basin, and the scour downstream the stilling basin. These characteristics will be tested in a pool-type stilling basin with negative and positive steps downstream of the sluice gate.

Forty-eight tests were carried out. For each test, the flow discharge (Q), the gate opening height (G), the thickness of the flow at vena-contracta (y_1), the conjugate depth of the jump (y_2), the length of the submerged jump (L_{sj}), and Froude number at vena-contracta (F_{r1}) were calculated. The experimental program was conducted on a re-circulating flume with 1.0 m wide, 26 m long, and 1.2 m deep, with a range of discharges range from 60 to 90 L/s. Regression analyses were performed, and equations were developed to correlate the length of the submerged jump with the other independent parameters. Finally, clear matching of results from the length of jump and velocity analysis was obtained and the optimal design for the stilling basin pool was identified.

Keywords: heading-up hydraulic structures, submerged hydraulic jump, sluice gate, Froude number

1. INTRODUCTION

Stilling basin provides means to absorb and dissipate the energy from the hydraulic structure discharge and protects the canal bed from scour. Stilling basin is one of the elements that cause a reduction of inflow velocity and energy. It is a very necessary element constructed downstream the hydraulic structures especially downstream low head structures, like barrages, weirs, dams, to dissipate the energy from these structure discharges and protects the canal from scouring which consequently protect the structure from failure.

Stilling basin is a short segment of a floored channel constructed downstream the gate where the flow downstream the hydraulic structure gate is supercritical flow and the hydraulic jump is formed. In this case, the supercritical flow, before reaching the canal bed, turns into a subcritical flow and great energy is dissipated; therefore, possible damage to the canal bed occurs.

Ali A. M. and Mohamed Y. A., [1], studied experimentally the effect of different shapes of stilling basins of a regulator on the length of the submerged hydraulic jump, velocity profiles along the apron, and local scour downstream the regulator floor. Chen J. et al, [2], conducted a 3-D numerical simulation for water flow in a stilling basin with multi-horizontal submerged jets using two different turbulent models called VOF RNG k- ϵ and Mixture RNG k- ϵ turbulence models. The results showed that the mathematical simulation could be used effectively to study the water flow and energy dissipation problems. It was found also that the mixture model covered a region about 18% larger than calculated by the VOF model. Abdelhaleem F. S. and Helal E., [3], studied experimentally the effect of using three different shapes of corrugated bed on characteristics of a hydraulic jump and downstream local scour for a wide range of Froude numbers ranging from 2.0 to 6.5. The results of the study confirmed the effectiveness of corrugated beds for energy dissipation downstream hydraulic structures

and decreasing the depth and length of the jump and thus reducing the stilling basins cost. Abdelhaleem F. S., [4], conducted an experimental study to predict the scour geometry downstream a Fayoum weir type and to minimize the scour using a row of different heights and positions semi-circular baffle blocks with different flow conditions. Pourabdollah N. et al, [5], studied experimentally and analytically the hydraulic jump characteristics on different adverse slopes, bed roughness, and positive step heights for Froude numbers ranging from 4 to 10. It was deduced that the decrease in sequent depth ratio and the increase in the relative energy loss were 33 and 27.41% more than those in the classic jump. Perez J. F. M. et al, [6], conducted experimentally on a physical model the characterization of the hydraulic jump profile and velocity distribution in a stilling basin. The free surface profile and velocity distribution of the developed hydraulic jump within the stilling basin structure were analyzed. It was found relevant variations for the hydraulic jump shape and the maximum velocity positions within the measured vertical profiles when compared to classical hydraulic jumps.

The present study aims to study the best design of stilling basin pool where it will investigate the effect of different locations and dimensions of stilling basin pools from regulator gates and study its effects on the characteristics of the submerged hydraulic jump, velocity profiles along the basin, and local scour downstream stilling basin floor. Experiments were conducted employing a wide range of Froude numbers, different tailwater depths, and different stilling basin locations and dimensions.

2. EXPERIMENTAL WORK

The experimental work was conducted in the laboratory of the Hydraulics Research Institute (HRI) of the National Water Research Center, Delta Barrage, Cairo, Egypt. A flume in general is a man-made open channel constructed over the ground to lead water from its source to its desired location. The experimental work was conducted using a physical model (flume) with dimensions of 1.0 m wide, 26.0 m long, and 1.20 m deep, as shown in Figure 1. The flume consisted of the inlet, exit, feeding system, the bed of the flume, the tailgate, and the main body, as illustrated in Figure 2. The flume sidewalls along the entire length of the flume were made of glass with steel frames to allow visual inspection of the flow patterns. The horizontal bottom of the flume was made of concrete and provided with a steel pipe to drain the water from the flume. The tailwater depth was controlled by a tailgate (control gate) located downstream of the flume.



Figure 1. Photo for the Side View of the Employed Flume

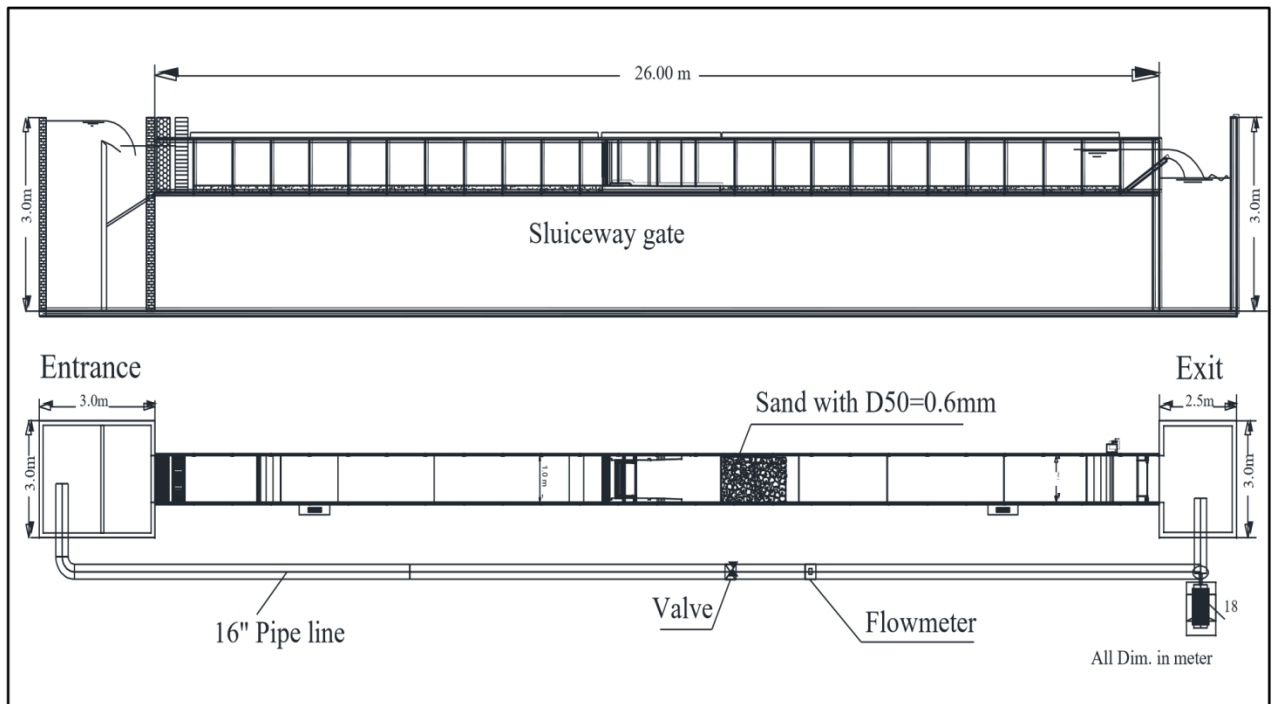


Figure 2. The Layout of the Flume

3. MEASUREMENTS

An electromagnetic flow-meter was used for measuring the discharge during the tests. The flow velocity profiles were measured at a different cross-section along the stilling

basin using an electromagnetic current-meter type EMS, manufactured by Delft Hydraulics, Holland. Moreover, an electromagnetic current meter was used to allocate the length of the submerged jump by tracing the positive and negative values of the flow velocity on the water surface layer. The zero-velocity point represented the length of the submerged hydraulic jump to the sluice gate. Different designs were experimentally tested. For each design, six different gate openings and different flow conditions were tested. Typical conditions used for experimental work for this research paper are provided in Table 1. Also, sketches for the studied cases are illustrated in Table 2. The discharge was 90 L/s, the flow velocity was measured at six cross-sections along the stilling basin. The first cross-section was located at a distance of 0.5 m downstream of the gate. The velocity profiles were measured at five points depth at relative distances from the surface 0.2, 0.4, 0.6, 0.8, and 0.9 of the total water depth.

4. METHODOLOGY

The research plan investigated the effect of selecting the location of the stilling basin pool at distances 30, 40, and 55 cm of a pool downstream the gate structure. The resistance of the pool on the energy dissipation and increasing or decreasing the scouring generated by the hydraulic jump were observed to determine the best location for the pool.

Table 1. The Experimental Program

Case	Location L_1 , cm	Length L_p , cm	Depth d , cm	Discharge Q , L/s	Gate Opening G , cm	Tailwater Depth y_t , cm	Submergence Ratio S_g
A	---	---	---	90	7 : 12	24.0 : 28.0	0.41 : 2.07
B	30	70	15	90	7 : 12	23.5 : 28.5	0.41 : 2.13
C	40	60	15	90	7 : 12	24.0 : 28.5	0.41 : 2.50
D	55	45	15	90	7 : 12	26.0 : 28.5	0.64 : 2.45
E	40	60	10	90	7 : 12	25.0 : 29.0	0.47 : 2.36
F	40	60	5	90	7 : 12	24.0 : 28.5	0.41 : 2.35
G	40	80	15	90	7 : 12	25.0 : 28.0	0.74 : 3.04

Table 2. Sketches for the Experimental Cases

Case A	Case B	Case C	Case D	Case E	Case F	Case G

After selecting the optimal location of the pool, the optimal dimensions of the pool were investigated concerning the cost, energy dissipation, and efforts of excavation by fixing L_1 (the distance from the gate to the beginning of the stilling basin) and changing L_p (the length of the pool) to 80, 70, 60, and 45 with the stability of d (the height of the pool); and thus the optimal length of the pool was determined. Then, the height d was changed to 15, 10, and 5 cm to determine the best height.

5. TEST PROGRAM

Eight different designs were conducted in the flume to reach the optimal stilling basin pool design concerning the maximum dissipation energy, the minimum scouring depth, and the best velocity decay distributions. For each design, six different gate openings were studied leading to different upstream and downstream water levels, different submerged ratios, different vena-contracta depths, and different

Froude numbers. Forty-eight tests were carried out. For each test, measurements were recorded for the flow discharges, the gate opening height, the conjugate and sequent depths of the jump, the jump length and height, and Froude numbers were also calculated.

6. RESULTS AND ANALYSES

The analysis procedures were categorized to investigate the length of the submerged hydraulic jump, the energy dissipation, near-bed velocity, and the scour downstream the stilling basin. The effect of stilling basin pool on the velocity distribution at different cross-sections along the stilling basin was also presented.

6.1 Effect of Stilling Basin Location (L_1)

This design included four cases (A, B, C, and D) where many parameters were analyzed and discussed such as the relative energy losses, length of the submerged hydraulic jump, and the scour bed downstream stilling basin. The location of stilling basin pool (L_1) had different values (30, 40, and 55 cm) to get the best location achieving the maximum energy dissipation and consequently the less scour depth.

6.1.1 Length of Submerged Hydraulic Jump

Figure 3 shows the relation between the relative length of the submerged jump (L_{sj}/L_B), L_{sj} is the length of the submerged hydraulic jump and L_B is the stilling basin length, and the Froude number (Fr_1) for different gate opening for cases A, B, C, and D. It can be observed that as the Froude number increased the relative length of submerged Jump decreased. Case D with gate opening 11 cm produced the highest value of the relative length of the submerged hydraulic jump compared to other cases. On the other hand, Case B with a gate opening 7 cm produced a small relative length of the submerged hydraulic jump. This means that the bigger gate opening resulted in bigger relative lengths of submerged hydraulic jump.

Regression analyses were performed for the different cases and equations were obtained on the figure to predict the relative length of the submerged hydraulic jump knowing Froude number Fr_1 .

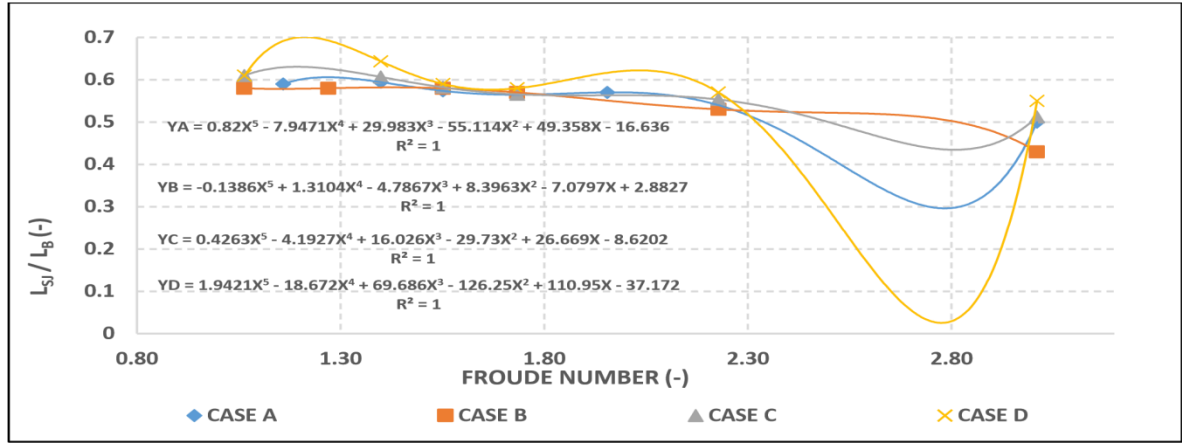


Figure 3. The Relation between Relative Length and Froude Number

6.1.2 Energy Dissipation

The energy loss was calculated between cross-section 1, which is located downstream of the sluice gate at the location of vena-contracta, and cross-section 2 at the end of the stilling basin through the hydraulic jump by applying the energy equation between upstream and downstream the stilling basin.

The energy losses at section 1 (at vena-contracta) were calculated by using the following formula:

$$E_1 = \psi + \frac{Fr_1^2}{2} \quad (1)$$

$$\Psi = \frac{y_3}{y_1} = \sqrt{\left(\frac{(1+S)^2}{4} (\Phi)^2 - 2Fr_1^2 + \frac{4Fr_1^2}{(1+S)(\Phi)} \right)} \quad (2)$$

$$\Phi = (1+8Fr_1^2)^{1/2} - 1 \quad (3)$$

Where: E_1 is the energy loss at the beginning of the submerged jump (at vena-contracta), Fr_1 is the Froude number, S_j is the submergence ratio = $(y_t - y_2)/y_2$, y_t is tailwater depth, and y_2 is the sequent water depth of the classical hydraulic jump. Also, the total energy losses between sections 1 and 2 were calculated by using the following formula, Rajaratnam, [7]

$$: E_L = \left(\psi - \frac{(1+S)}{2} \Phi \right) + \frac{Fr_1^2}{2} \left(1 - \frac{4}{(1+S)^2 (\Phi)^2} \right) \quad (4)$$

Also, the relative energy loss ($E_L/E_1 * 100$) can be given assuming a horizontal apron as:

$$\Delta E = \frac{E_L}{E_1} = \frac{\left(\psi - \frac{(1+S)}{2} \Phi \right) + \frac{Fr_1^2}{2} \left(1 - \frac{4}{(1+S)^2 (\Phi)^2} \right)}{\psi + \frac{Fr_1^2}{2}} \quad (5)$$

The relation between the relative energy loss and Froude number Fr_1 is shown in Figure

4. Regression analyses were performed for the different cases and equations were obtained on the figure to predict the energy loss of the submerged hydraulic jump knowing Froude number Fr_1 .

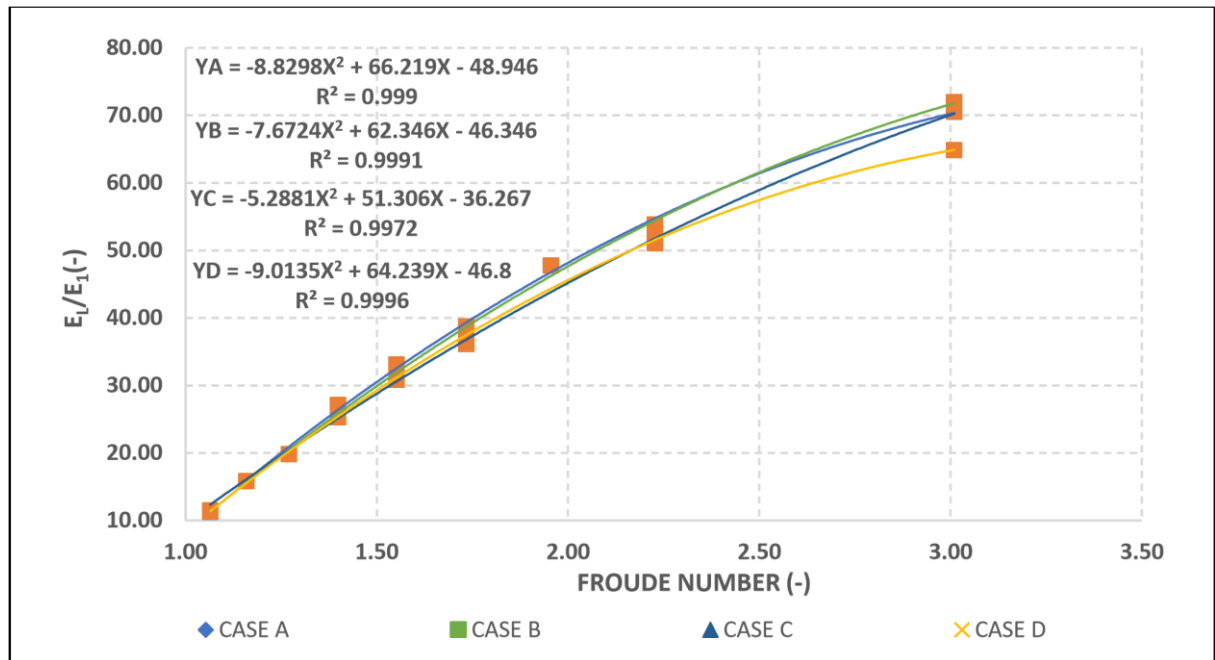


Figure 4. The Relation between Energy Losses and Froude Number

6.1.3 Scour Downstream the Stilling Basin

Figure 5 shows the relation between the relative scour depth Ds/y_{calc} and the Froude number Fr_1 for different gate opening of cases A, B, C, and D. Case C produced the smallest value of scour depth compared to other cases. On the other hand, Cases A and B produced the highest values of scour depth. Regression analyses were performed for the different cases and equations were obtained on the figure to predict the relative scour depth of the submerged hydraulic jump knowing Froude number Fr_1 .

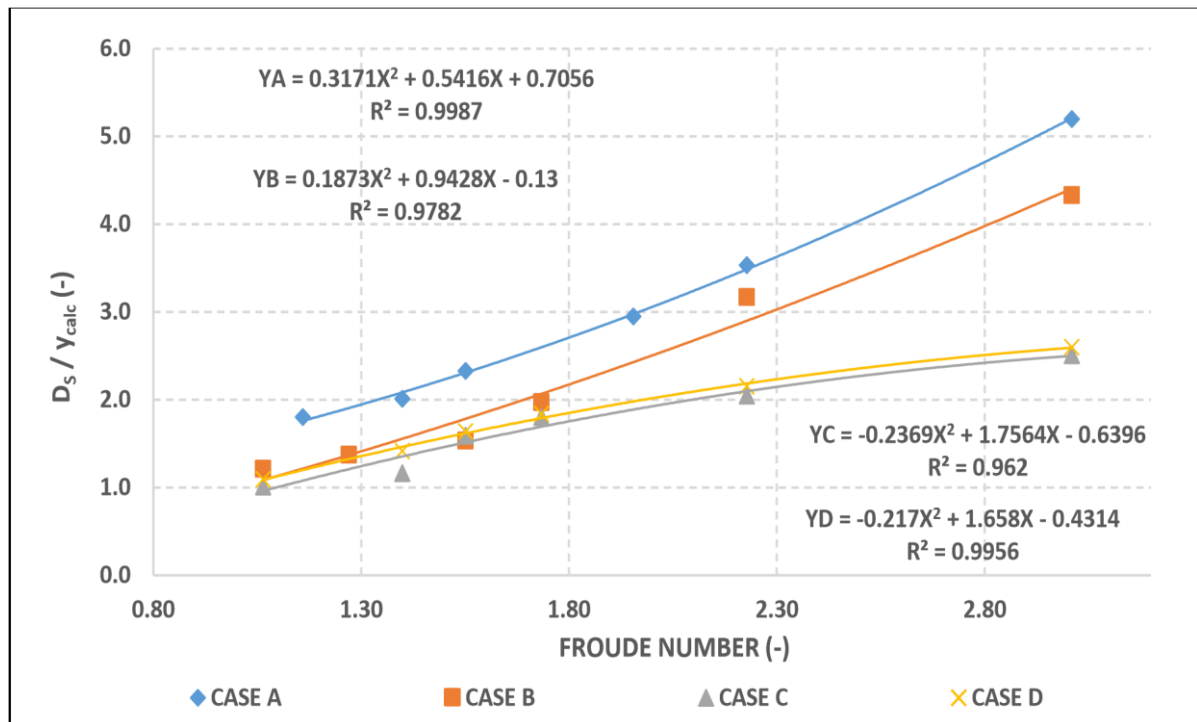


Figure 5. Relationship between Relative Scour Depth and Froude Number

6.2 Effect of Stilling Basin Pool Length (L_p)

This design included five cases (A, B, C, D, and G). The length of stilling basin pool had various values of 80, 70, 60, and 45 cm to get the best length giving the maximum energy dissipation and consequently the less scour depth.

6.2.1 Length of submerged Hydraulic Jump

Figure 6 shows the relation between the relative length of the submerged jump (L_{sj}/L_B) and the Froude number (Fr_1) for different gate openings. Case D produced the highest value of the relative length of the submerged hydraulic jump (L_{sj}/L_B) compared to other cases. On the other hand, Case B produced a small relative length of the submerged hydraulic jump.

Regression analyses were performed for the different cases and equations were obtained on the figure to predict the relative length of the submerged hydraulic jump knowing Froude number Fr_1 .

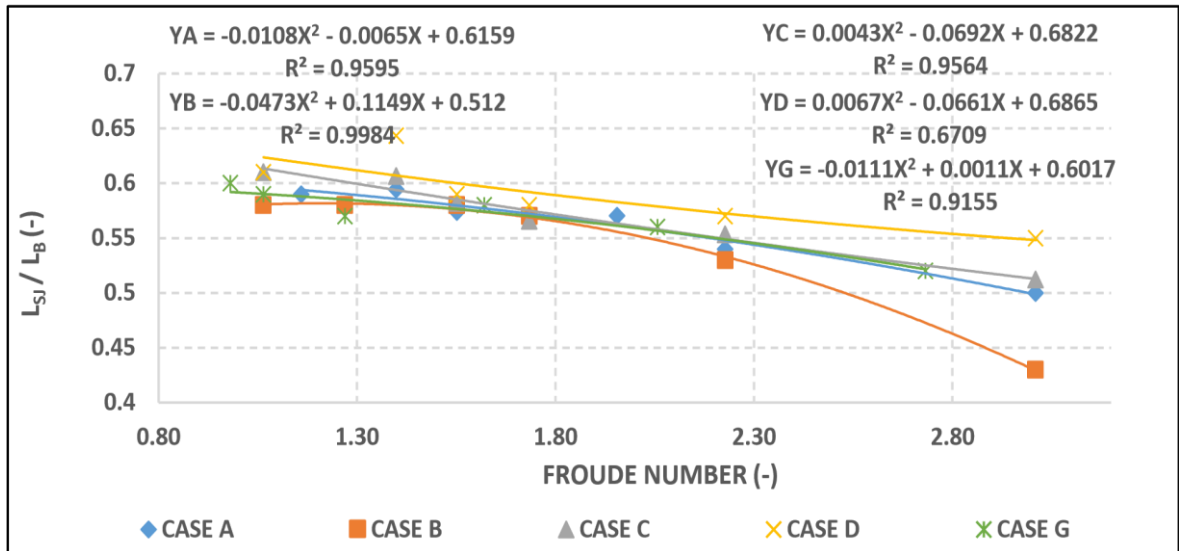


Figure 6. Relationship between Relative Length of submerged Hydraulic Jump and Fr_1

6.2.2 The Relative Energy Losses

Figure 7 shows the relation between the Froude number (Fr_1) and the relative energy losses (E_l/E_1). Cases D and G had the lowest values of relative energy losses compared to other cases. On the other hand, Cases A, B, and C had the highest values of relative energy losses.

Regression analyses were performed for the different cases and equations were obtained on the figure to predict the energy loss of the submerged hydraulic jump knowing Froude number Fr_1 .

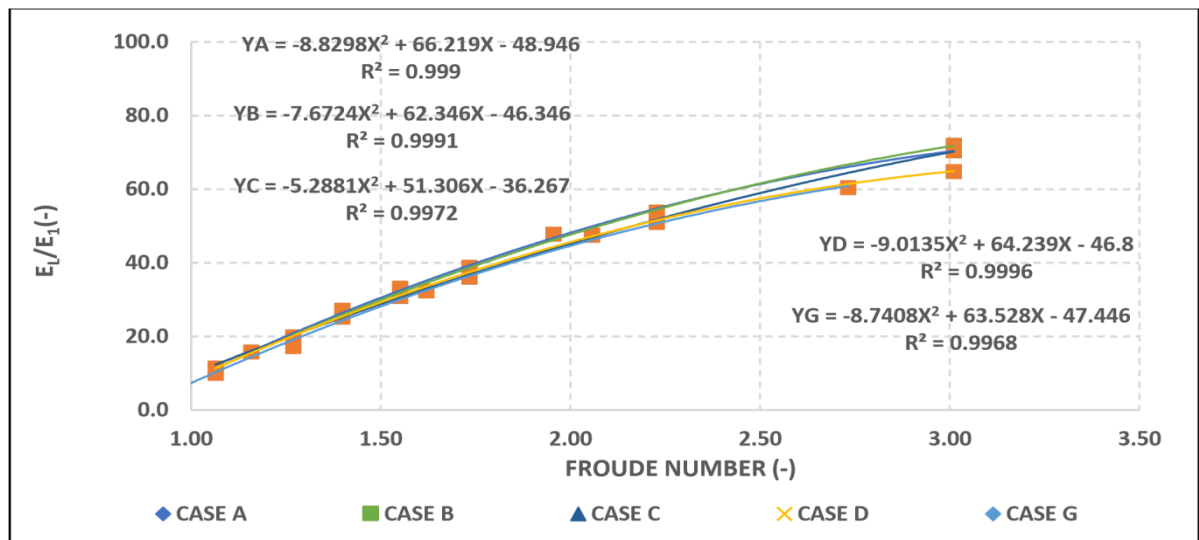


Figure 7. Relationship between Relative Energy Losses and Froude Number

6.2.3 The Scour Downstream the Stilling Basin

Figure 8 shows the relation between the Froude number (Fr_1) and the relative scour depth D_s/y_{calc} . Case G produced the smallest value of scour depth compared to other cases. On the other hand, cases A and B had the lowest values of scour depths.

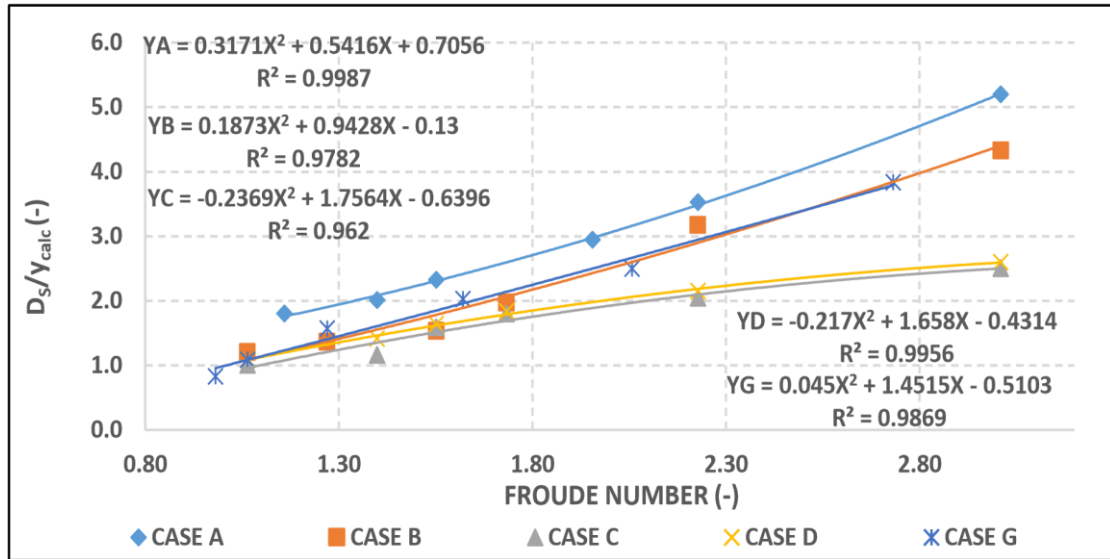


Figure 8. Relationship between Relative Depth and Froude Number

Regression analyses were performed for the different cases and equations were obtained on the figure to predict the relative scour depth of the submerged hydraulic jump knowing Froude number Fr_1 .

6.3 Effect of Stilling Basin Pool Depth (d)

This design included four cases (A, C, E, and F). The depth of stilling basin pool had different values of 15, 10, and 5 cm to get the best depth giving the maximum energy dissipation and consequently the less scour depth.

6.3.1 Length of submerged Hydraulic Jump

Figure 9 shows the relationship between the Froude number (Fr_1) and the length of the submerged hydraulic jump. The maximum length of the submerged jump was found at Case F where the stilling basin pool depth was 5 cm, while the minimum length of the submerged jump was found at Case C where the stilling basin pool depth was 15 cm. Regression analyses were performed for the different cases and equations were obtained on the figure to predict the relative length of the submerged hydraulic jump knowing Froude number Fr_1 .

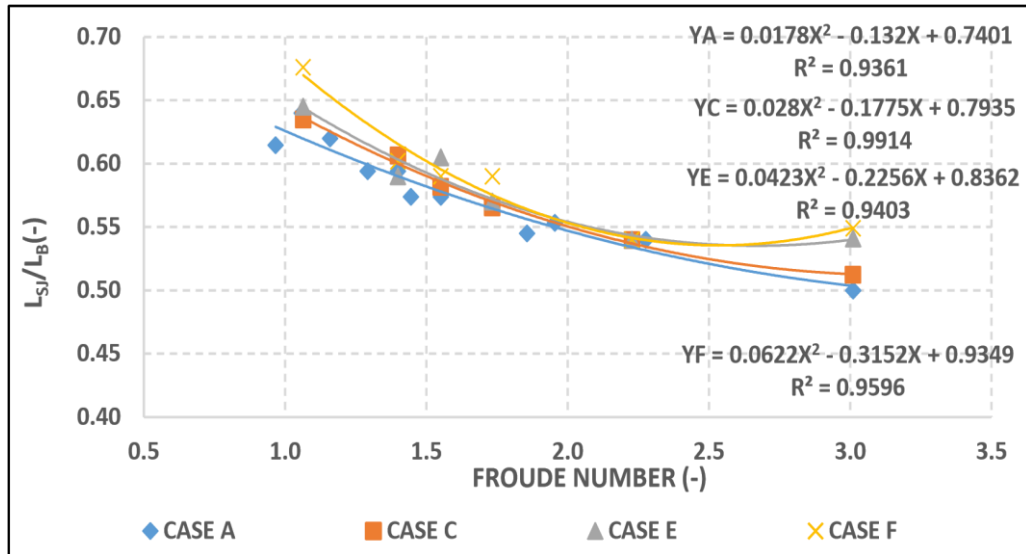


Figure 9. Relationship between Length of Submerged Hydraulic Jump and Fr_1

6.3.2 The Relative Energy Losses

Figure 10 shows the relation between the Froude number (Fr_1) and the relative energy losses. The energy losses accompanied with scouring depth were desirable in Case C, although very close to Cases E and F.

Regression analyses were performed for the different cases and equations were obtained on the figure to predict the energy loss of the submerged hydraulic jump knowing Froude number Fr_1 .

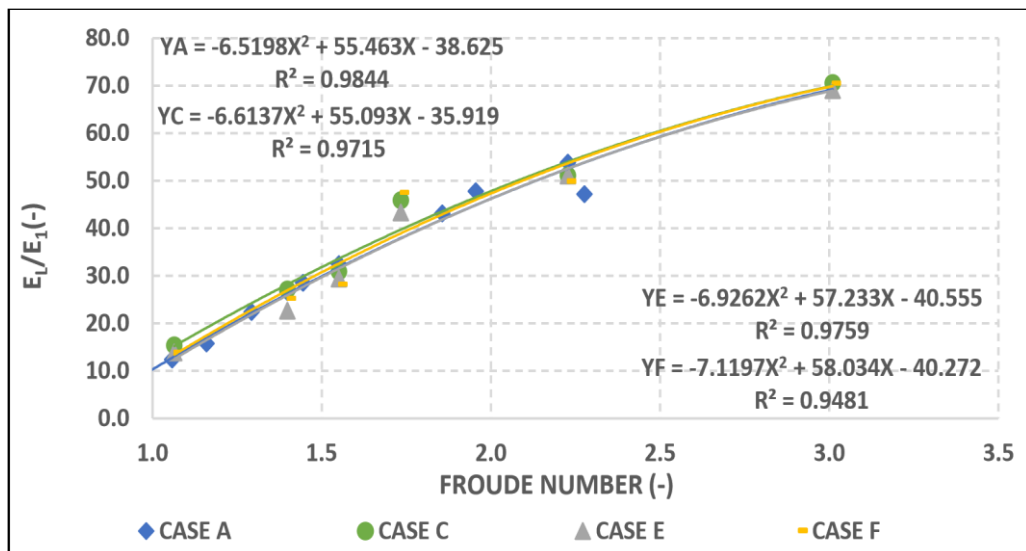


Figure 10. Relationship between Relative Energy Losses and Fr_1

6.3.3 The Scour Downstream the Stilling Basin

Figure 11 shows the relation between the scour depth D_s/y_{calc} and the Froude number Fr_1 for different gate openings for cases A, C, E, and F. Case (C) produced the smallest value of scour depth compared to other cases. On the other hand, Case F produced the highest value of scour depth.

Regression analyses were performed for the different cases and equations were obtained on the figure to predict the relative scour depth of the submerged hydraulic jump knowing Froude number Fr_1 .

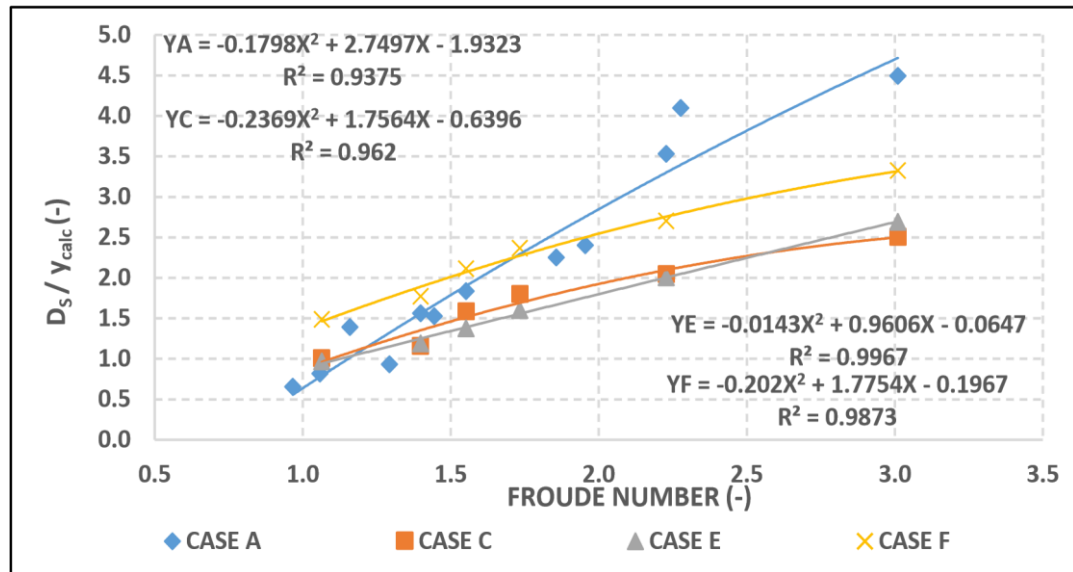


Figure 11. Relationship between Scour Depth and Fr_1

7. CONCLUSIONS

The most important outputs of this study can be summarized as follows:

1. It was found that for all different gate openings, design C was the best case achieving maximum energy dissipation and minimum scour depth.
2. Design B was very close to design C concerning the amount of energy dissipation, but the scour depth was a little more.
3. Design D gave a little longer submerged jump length than design C but with less dissipation energy value and a little more scour depth.
4. Design C achieved scour depth less than normal case (without stilling basin) with 25%.
5. For applying in prototype, Design C should have a relative length (L_1/L_B) equal to 4, where L_1 is the distance between gate opening and beginning of the pool and L_B is the stilling basin length.
6. For applying in prototype, Design C should have a relative length (L_p/L_B) equal to 60%, where L_p is the length of the pool and L_B is the stilling basin length.
7. Design C has an economic application compared to the other investigated designs (A, B, D, E, F, and G).

8. REFERENCES

1. Ali A. M., and Mohamed Y.A. (2010). "Effect of Stilling Basin Shape on the Hydraulic Characteristics of the Flow Downstream Radial Gates". Alexandria Engineering Journal, ELSEVIER, No. 49, pp. 393-400, Alexandria, Egypt.
2. Chen J., Zhang J., Xu W., and Wang Y. (2010). "Numerical Simulation of the Energy Dissipation Characteristics in Stilling Basin of Multi-Horizontal Submerged Jets". Journal of Hydrodynamics, JHD, ELSEVIER, Scencedirect.com/science/journal/10016058, 732-741
3. Abdelhaleem F. S., Amin A. M., and Helal E. Y. (2012). "Effect of Corrugated Bed Shapes on Hydraulic Jump and Downstream Local Scour". Journal of American Science; 8(5): 1-10, ISSN: 1545-1003.
4. Abdelhaleem F. S. (2013). "Effect of Semi-Circular Baffle Blocks on Local Scour Downstream Clear-Overfall Weirs", Ain Shams Engineering Journal, ELSEVIER, No. 4, pp. 675-684, Alexandria, Egypt.
5. Pourabdollah, N., Heidarpour M., and Koupai J. A. (2019). "An Experimental and Analytical Study of a Hydraulic Jump over a Rough Bed with an Adverse Slope and Positive Step". Iranian Journal of Science and Technology, Transaction of Civil Engineering, No. 43, pp. 551-561, Iran.
6. Perez, J. F. M., Moran F. J., Gomez S. S., Estrada M. De., and Bartual R. G. (2020). "Experimental Characterization of the Hydraulic Jump Profile and Velocity Distribution in a Stilling Basin Physical Model". Water Journal, MDPI, 12, 1758; doi:10.3390/w 12061758.
7. Rajaratnam, N. (1965). "Submerged Hydraulic Jump". Journal of the Hydraulics Div.,